

# Recycling Upstream Redox Enzymes Expands the Regioselectivity of Cycloaddition in Pseudo-Aspidosperma Alkaloid Biosynthesis

Mohamed O. Kamileen, Matthew D. DeMars II, Benke Hong, Yoko Nakamura, Christian Paetz, Benjamin R. Lichman, Prashant D. Sonawane, Lorenzo Caputi,\* and Sarah E. O'Connor\*



Cite This: *J. Am. Chem. Soc.* 2022, 144, 19673–19679



Read Online

ACCESS |



Metrics & More



Article Recommendations



Supporting Information

**ABSTRACT:** Nature uses cycloaddition reactions to generate complex natural product scaffolds. Dehydrosecodine is a highly reactive biosynthetic intermediate that undergoes cycloaddition to generate several alkaloid scaffolds that are the precursors to pharmacologically important compounds such as vinblastine and ibogaine. Here we report how dehydrosecodine can be subjected to redox chemistry, which in turn allows cycloaddition reactions with alternative regioselectivity. By incubating dehydrosecodine with reductase and oxidase biosynthetic enzymes that act upstream in the pathway, we can access the rare pseudoaspidosperma alkaloids pseudo-tabersonine and pseudo-vincadifformine, both *in vitro* and by reconstitution in the plant *Nicotiana benthamiana* from an upstream intermediate. We propose a stepwise mechanism to explain the formation of the pseudo-tabersonine scaffold by structurally characterizing enzyme intermediates and by monitoring the incorporation of deuterium labels. This discovery highlights how plants use redox enzymes to enantioselectively generate new scaffolds from common precursors.

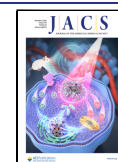
Alkaloid-producing plants in the Apocynaceae family have evolved cyclases that catalyze the cycloaddition of a highly reactive substrate, dehydrosecodine (**1**), into distinct alkaloid scaffolds.<sup>1,2</sup> We and others recently discovered and characterized the only known enzymes that catalyze cycloaddition of **1**: tabersonine synthase (*TiTabS* and *CrTS*), which catalyzes the formation of (–)-tabersonine (**2**) (precursor to anticancer drugs vinblastine and vincristine), catharanthine synthase (*CrCS*), which catalyzes formation of (+)-catharanthine (**3**) (precursor to vinblastine and vincristine), and coronaridine synthase (*TiCorS*), which catalyzes formation of (–)-coronaridine (**4**) (precursor to antiaddiction agent ibogaine) (Figure 1).<sup>2–5</sup> *TiTabS/CrTS* and *CrCS* directly yield **2** and **3** from **1** by a formal [4+2] cycloaddition,<sup>2,6</sup> while *TiCorS* initially forms a hitherto uncharacterized unstable intermediate, which is then enzymatically reduced to **4**. The **1** substrate could, in principle, undergo alternative cycloaddition reactions to yield additional scaffolds, but extensive mutagenesis of these cyclases did not result in an expansion of the enzymatic product profile.<sup>2</sup> Here we show that the cyclase *TiCorS* can, in addition to generating **4**, also produce the alternative pseudo-aspidosperma (Ψ-aspidosperma)-type alkaloid pseudo-tabersonine (Ψ-tabersonine) (**5**) (Figure 1). We show the mechanistic basis behind this transformation by first characterizing the unstable intermediate produced by the cyclase *TiCorS*. This intermediate can be intercepted by a reductase to generate **4** or by both a reductase and an oxidase to generate the alternative scaffold **5**. Deuterium labeling provides evidence for the mechanism of these enzymatic transformations. In short, the chemical reactivity of **1** is exploited by both a cyclase and a pair of redox enzymes that can isomerize the alkene moieties, which in turn facilitates new cyclization regioselectivity.

*Tabernanthe iboga*, a plant that produces **2** and **4** via enzymes *TiTabS* and *TiCorS*, respectively,<sup>3</sup> also produces Ψ-aspidosperma-type alkaloid 20-*epi*-ibophyllidine (Figure 1).<sup>7–9</sup> We hypothesized that **5** would be the precursor to 20-*epi*-ibophyllidine.<sup>10</sup> The natural product **5**, rarely observed in nature, has only been isolated from *Tabernaemontana calcaria*, a species closely related to *T. iboga*.<sup>11,12</sup> To identify *T. iboga* enzymes that could form (+)-Ψ-tabersonine **5**, we performed coupled *in vitro* biochemical assays in which the unstable **1** substrate is enzymatically generated from the upstream intermediate stemmadenine acetate (**6**). **6** is first oxidized by the flavin-dependent enzyme precondylocarpine acetate synthase (*PAS*)<sup>5</sup> to generate precondylocarpine acetate (**7**) and then undergoes a 1,4-iminium reduction by the medium chain alcohol dehydrogenase dihydroprecondylocarpine acetate synthase (*DPAS*) (Figure 1).<sup>13</sup> The resulting reduced unstable product, dihydroprecondylocarpine acetate (**8**), undergoes elimination of an acetoxy group to yield **1**, which is then captured by one of the cyclases (Figure 1).

Our initial hypothesis was that a dedicated cyclase in *T. iboga* would catalyze isomerization and cyclization of **1** to **5**. The *T. iboga* transcriptome, which contains the two previously identified cyclases *TiTabS* and *TiCorS* (81% sequence identity, Figure S1), does not harbor any additional cyclase homologues that might have alternative cyclization specificity. However, to our surprise, we observed that under certain conditions, **5**,

Received: August 1, 2022

Published: October 14, 2022



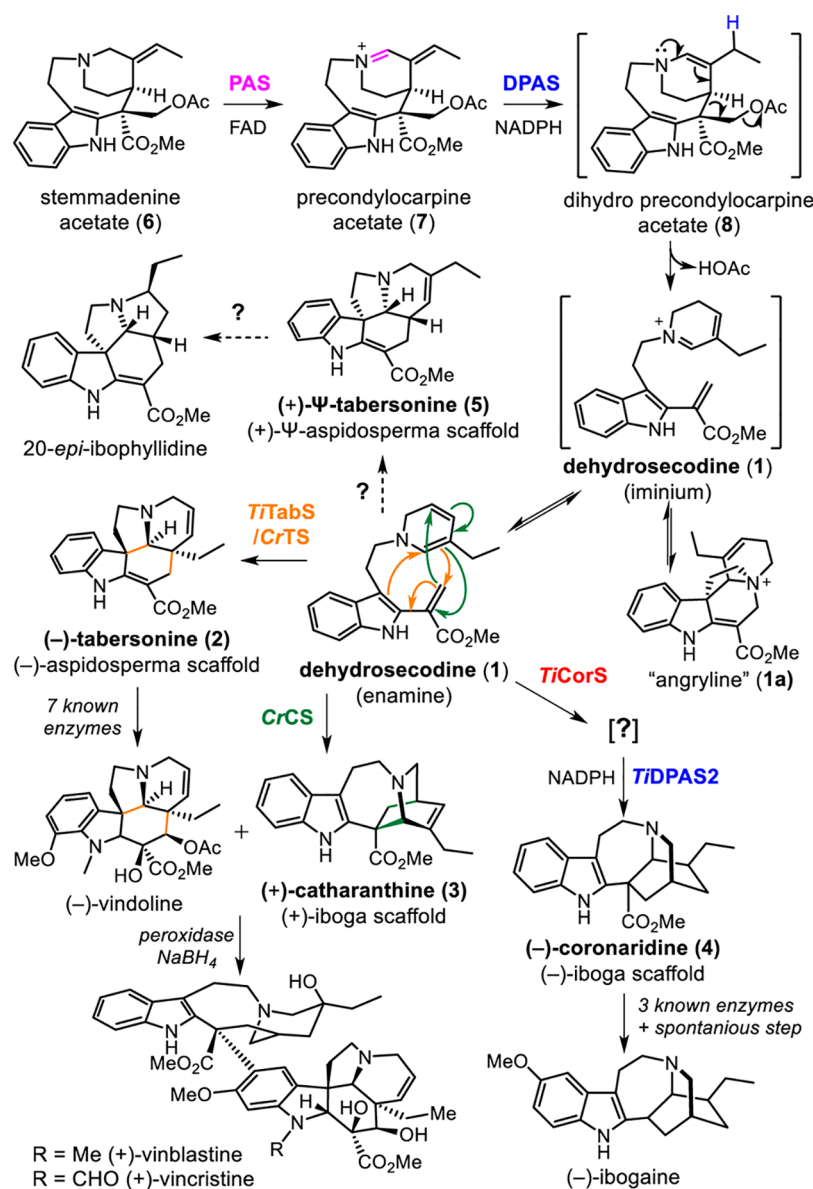


**Figure 1.** Dehydrosecodine (1)-derived alkaloids produced by the Apocynaceae family of plants.

rather than 4, was formed in assays using *TiCorS* (Figure 2a). Therefore, *TiCorS* appears to be involved in production of both 4 and 5.

*In vitro* assays using heterologously produced proteins (Figure S2) were used to probe the conditions that led to a switch in product selectivity. We first noted that the use of specific homologues of reductase DPAS and oxidase PAS with *TiCorS* led to changes in the product profile. *T. iboga* has two homologues of the reductase DPAS (*TiDPAS1*, *TiDPAS2*, Figure S3) and three homologues of PAS (*TiPAS1*, *TiPAS2*, *TiPAS3*, Figure S4).<sup>3</sup> Additionally, a PAS homologue (*CrPAS*)<sup>5</sup> from the taxonomically related plant, *Catharanthus roseus*, which produces vinblastine, is also available and was tested. Most importantly, the pH of the reaction was critical, with 5 formation being observed at pH 7.5 and 4 production observed at pH 9.5 (Figures S5 and S6). Overall, 5 formation was favored at pH 7.5, with *TiPAS1–3* or *CrPAS*, *TiDPAS1*, and *TiCorS*, 2 production was favored at pH 7.5, with *TiPAS1–3* or *CrPAS*, *TiDPAS1*, and *TiCorS*, and 4 formation was favored at pH 9.5 with *TiPAS1–3*, *TiDPAS2*, and *TiCorS*

(Figure 2a and Figures S5 and S6). Additionally, we also could produce the over-reduced version of 5, pseudo-vincadifformine ( $\Psi$ -vincadifformine) (9), by using *TiPAS1–3* (instead of *CrPAS*), *TiDPAS1*, and *TiCorS* (Figure 2a and Figure S7).

To further substantiate the results obtained *in vitro*, we reconstituted the biosynthetic enzymes reported here, leading to the production of 2, 5, and 9 in *Nicotiana benthamiana*. Enzymes were transiently expressed in *N. benthamiana* leaves, disks were excised from the transformed leaf tissue, and these disks were placed in buffer containing 6 (Figure 2b). We observed the production of 2, 5, and 9 in the extracts of the leaf disks using this expression system (Figure 2b). 4 was not detected in any of the enzyme combinations tested in *N. benthamiana*, presumably because of the higher pH conditions required for formation of this product. Additionally, the selectivity observed for the PAS homologues was not observed *in planta*, because *N. benthamiana* harbors an endogenous enzyme that is able to oxidize substrate 6 (Figure 2b).<sup>5</sup>

An acid-stable isomer of dehydrosecodine, angryline (1a), can also be isolated and directly used in cyclization assays

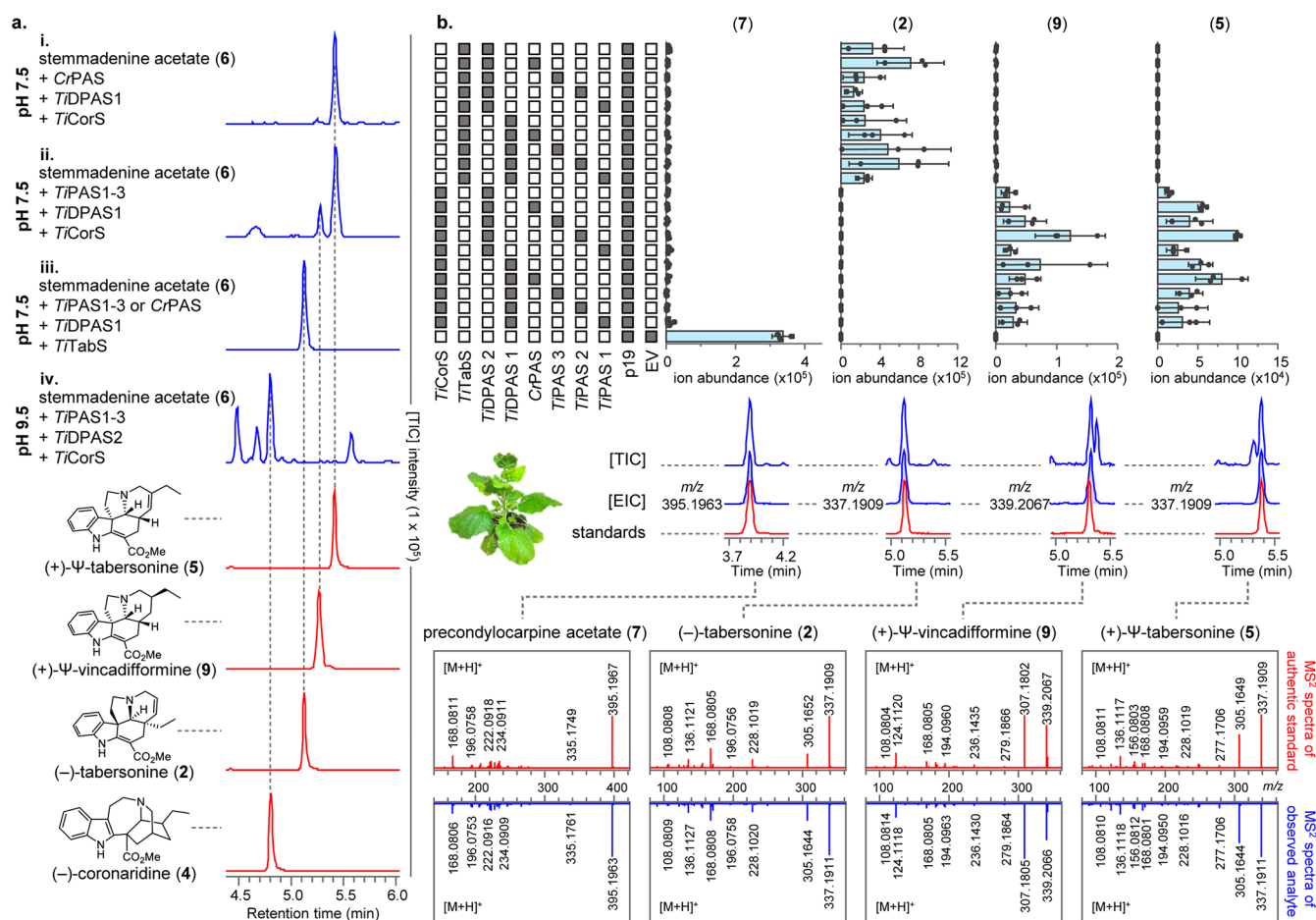


**Figure 2.** Biosynthesis of  $\Psi$ -tabersonine (5). (a) *In vitro* production of (i) (+)- $\Psi$ -tabersonine (5), (ii) (+)- $\Psi$ -vincadifformine (9), (iii) (-)-tabersonine (2), and (iv) (-)-coronaridine (4). (b) Reconstitution of  $\Psi$ -tabersonine (5) biosynthesis in *N. benthamiana* from stemmadenine acetate (6). Pathway enzyme combinations (filled gray boxes) transiently expressed in *N. benthamiana* and harvested leaf disks fed with stemmadenine acetate (6) and the resulting levels of precondylocarpine acetate (7), (-)-tabersonine (2),  $\Psi$ -vincadifformine (9), and  $\Psi$ -tabersonine (5) (bars represent  $\pm$  S.E.). Representative TIC and EIC for the products observed in *N. benthamiana* reconstitution along with authentic standards and MS<sup>2</sup> fragmentation spectra are shown.

(Figure 1).<sup>2</sup> **1a** must be used at a pH value above 8.5, where it will open to generate the reactive **1**. When **1a** was used in enzymatic assays in place of **6** (pH 9.5), we could observe formation of **5**, **2**, **4**, and **9** (Figure S8). Notably, both PAS (*TiPAS1*–*3*, *CrPAS*) and *TiDPAS1* were required for the formation of **5** and **9**, indicating that these enzymes are required for the formation of the  $\Psi$ -aspidosperma scaffold. PAS was not required for **4** production, which was favored when reductase *TiDPAS2* was used (Figures S9 and S10).

To investigate the mechanism by which *TiCorS* can act, we first set out to characterize the initial, unstable product that is released from *TiCorS* in the absence of reductase (Figure 1). We optimized conditions under which this intermediate could be isolated and reductively trapped this compound with NaBH<sub>4</sub>. NMR analysis showed that the compound was 16-carbomethoxycleavamine (**10**), suggesting that the initial cyclization product of *TiCorS* is 16-carbomethoxycleaviminium (**11**) (Figure 3 and Figure S11). When the *TiCorS* product was reduced with NaBD<sub>4</sub>, the deuterium label was incorporated at carbon 21, **10-d**, which would be expected for 1,2-reduction of **11** (Figure 3). Notably, the crystal structure of related cyclase *CrCS* (70.8% sequence identity, Figure S1) showed that *CS* initially forms (+)-16-carbomethoxycleaviminium (**11a**),<sup>14</sup> which then subsequently cyclizes to **3**,

though unlike *TiCorS*, the intermediate is not released from the active site.<sup>2</sup> Moreover **3** can open to form **11a** under acidic conditions (Figure S12).<sup>1,2,15</sup> We used CD spectroscopy to show that *TiCorS* generates (-)-16-carbomethoxycleavamine (**10**), which is the opposite enantiomer that is generated by *CrCS* (Figure S13).

With knowledge of the cyclization product of *TiCorS*, we proposed a mechanism for the formation of **4**. After release from the active site of *TiCorS*, **11** undergoes a 1,4-reduction by *TiDPAS2*, which in turn would facilitate a second cyclization to form **4** (Figure 4). We speculate that at higher pH values, *TiDPAS2* favors 1,4-reduction, which when followed by tautomerization,<sup>16</sup> primes the substrate to cyclize to **4**.

However, the mechanism by which **11** could be transformed into the **5** scaffold was still not clear. Therefore, we performed the reaction in the presence of isotopically labeled NADPH (pro-(*R*)-NADPD) to determine where the deuteride is incorporated in **5**.<sup>13,17,18</sup> We incubated **6** with *CrPAS*, *TiDPAS1*, and *TiCorS* or *TiTabS*, along with pro-(*R*)-NADPD, which is required for DPAS reduction (Figure S14). With *TiTabS*, we saw formation of the **2** product with a mass consistent with incorporation of one deuterium, as expected from the action of DPAS acting on **7** (Figure 4).<sup>13</sup> However, when *TiCorS* was substituted for *TiTabS*, the

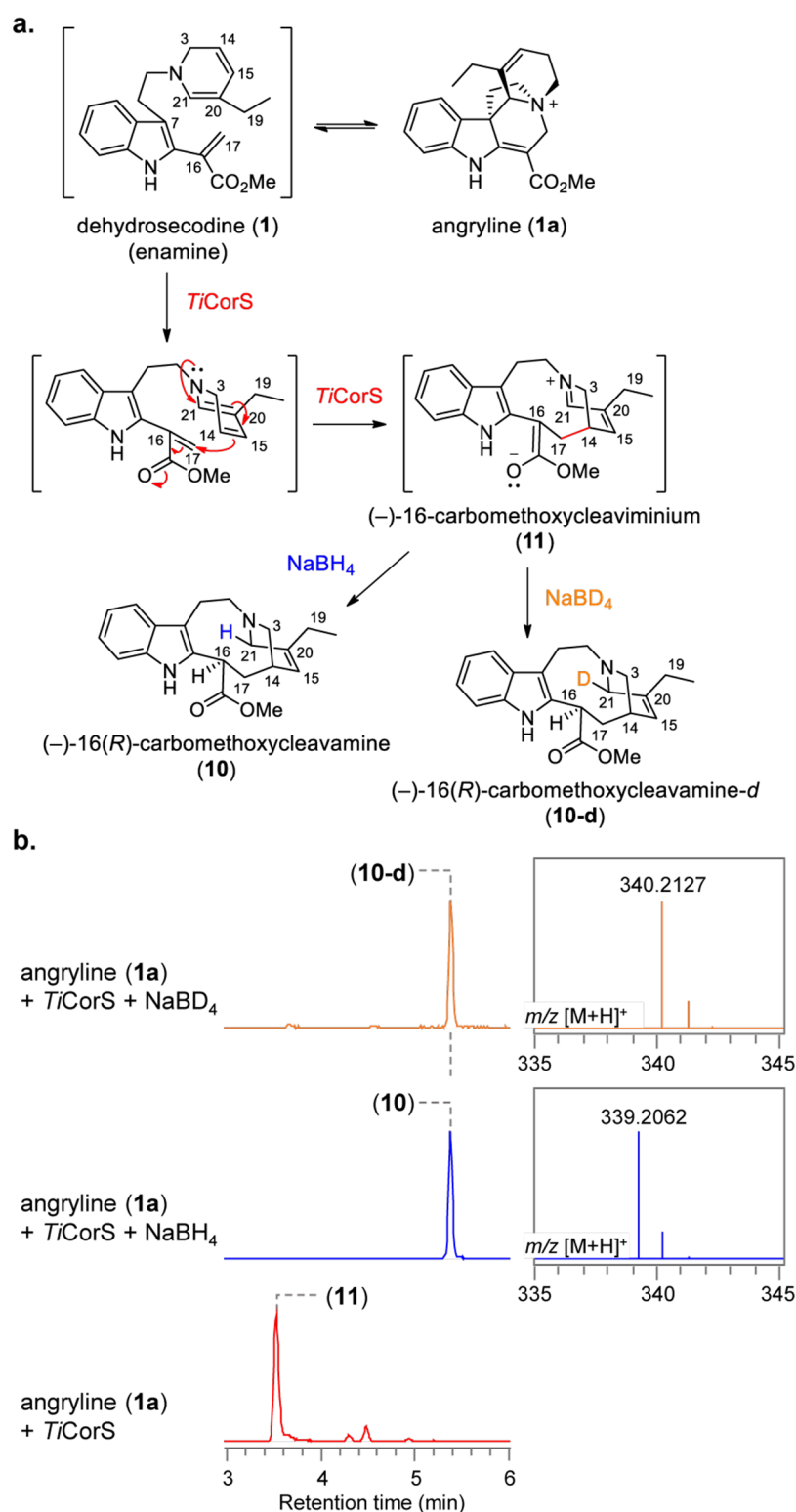


**Figure 3.** Formation of 16-carbomethoxycleavamine (**10**). (a) *TiCorS* generates 16-carbomethoxycleaviminium (**11**), which could be trapped by NaBH<sub>4</sub> to generate 16-carbomethoxycleavamine (**10**) or NaBD<sub>4</sub> to generate 16-carbomethoxycleavamine-*d* (**10-d**). (b) TIC and MS spectra representing the formation of 16-carbomethoxycleaviminium (**11**) and 16-carbomethoxycleavamine (**10**) or 16-carbomethoxycleavamine-*d* (**10-d**).

resulting **5** product had a mass consistent with incorporation of two deuterium atoms (Figure 4 and Figure S14), clearly demonstrating that formation of **5** from **6** requires two reduction steps. Furthermore, the **9** product showed a mass incorporation of three deuterium atoms (Figure 4 and Figure S14). To corroborate these results, we also incubated the

trapped isomer of **1**, **1a** with PAS, *TiDPAS1*, the labeled NADPD cofactor, and *TiTabS* or *TiCorS*. The **2** product produced by *TiTabS* had no deuterium incorporation, as expected; formation of **5** and **9** from **1a** showed incorporation of one and two deuterium atoms, respectively, and was strictly

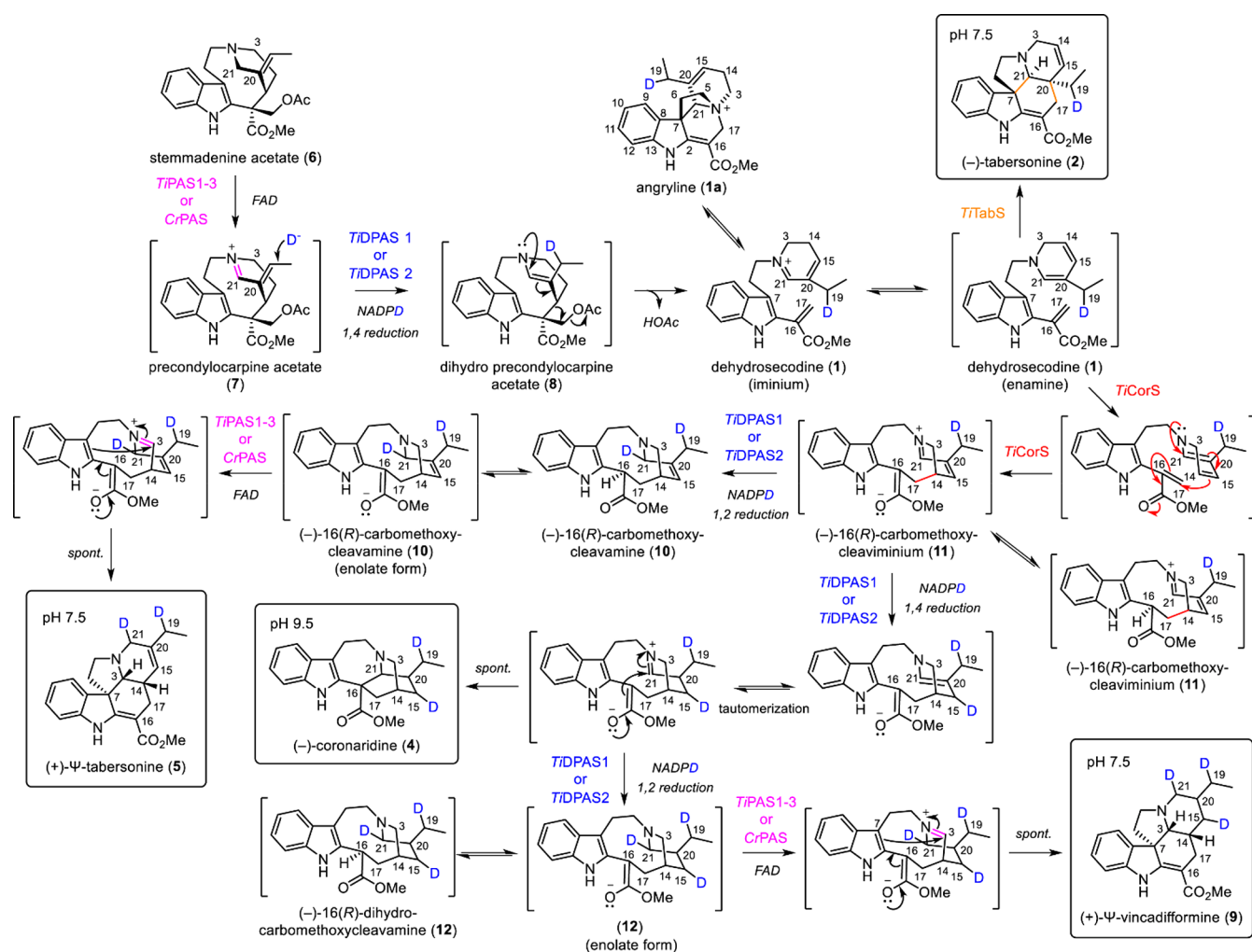


**Figure 4.** Proposed mechanism for the formation of (–)-iboga and (+)-Ψ-aspidosperma alkaloids. Biosynthesis of (–)-iboga alkaloid (–)-coronaridine (4) and Ψ-aspidosperma alkaloids (+)-Ψ-tabersonine (5) and (+)-Ψ-vincadifformine (9) with deuterium (blue) tracers using isotopically labeled NADPD.

dependent upon the presence of both reductase, *TiDPAS1*, and oxidase, *PAS* (Figure S15).

We isolated isotopically labeled 2, 5, and 9 and showed that the deuterium labels were incorporated at carbon 19 for 2 as expected,<sup>13</sup> and carbons 19 and 21 for 5, carbons 19, 21, and 15 for 9 (Figure 4). We performed CD spectroscopy of these isolated products and assigned the stereochemistry as (+)-Ψ-tabersonine (5) and (+)-Ψ-vincadifformine (9), which is the expected stereochemistry based on the downstream ibophyllidine products (Figure S16). Finally, we incubated the chemically 1,2-reduced *TiCorS* product, 10, with the oxidase *PAS* and observed formation of 5 (Figure 4 and Figure S17), indicating that cyclization occurs after *PAS*-catalyzed oxidation.

Together, this evidence strongly supports a mechanism for the formation of 5 (Figure 4). *TiCorS* cyclizes 1 to 11 and releases it from the active site, where it is reduced to 10 via 1,2-reduction by *TiDPAS1* and then reoxidized by *PAS*. The resulting intermediate is then primed to spontaneously cyclize to form 5. 9 forms by *PAS* oxidation of the doubly reduced (–)-16-dihydrocarbomethoxy-cleavamine (12) (Figure 4 and Figure S7). The switch between 4 and 5 is ultimately controlled by whether *DPAS* catalyzes a 1,4-reduction or 1,2-reduction. The changes in the assay pH conditions or protein–protein interactions may be responsible for favoring 1,2-

reduction over 1,4-reduction. Alternatively, an as yet undiscovered reductase that generates 4 at physiological pH may be responsible for the biosynthesis of this compound in *T. iboga*.

We hypothesized that the (+)-16-carbomethoxy-cleavamine (10a) intermediate generated from opening of 3 could serve as a precursor to (–)-Ψ-tabersonine (5a).<sup>19</sup> However, oxidation of (+)-16-carbomethoxy-cleavamine (10a) by *PAS* yielded only a small amount of product, which, although having a mass and retention time consistent with (+)-Ψ-tabersonine 5, could not be fully characterized (Figure S17). Thus, *PAS* may only recognize one 16-carbomethoxy-cleavamine enantiomer.

Here we show how redox transformations of dehydrosecodine (1) enable cycloaddition reactions with alternative regioselectivity to form (–)-coronaridine (4), (+)-Ψ-tabersonine (5), or (+)-Ψ-vincadifformine (9). Notably, these redox enzymes, *DPAS* and *PAS*, which transform stemmadenine acetate (6) into dehydrosecodine (1), are recruited from upstream in the biosynthetic pathway. Therefore, this discovery highlights how plants can recycle enzymes for use in more than one pathway step. Future studies are required to establish how the recruitment of these upstream enzymes is controlled. Nevertheless, the detailed chemical analyses described here provide a compelling hypothesis for the

mechanism by which these redox reactions and subsequent cyclizations expand the number of scaffolds produced from the versatile dehydrosecodine (1) intermediate.

## ■ ASSOCIATED CONTENT

### SI Supporting Information

The Supporting Information is available free of charge at <https://pubs.acs.org/doi/10.1021/jacs.2c08107>.

Additional experimental details, assays, materials, and methods, and NMR spectra described in this study (PDF)

### Accession Codes

GenBank accession numbers: MH213134 (CrPAS), MK840850 (TiPAS1); MK840851 (TiPAS2); MK840852 (TiPAS3); MK840853 (TiTabS); MK840854 (TiCorS); MK840855 (TiD-PAS1); MK840856 (TiDPAS2).

## ■ AUTHOR INFORMATION

### Corresponding Authors

**Sarah E. O'Connor** – Department of Natural Product Biosynthesis, Max Planck Institute for Chemical Ecology, Jena 07745, Germany; [orcid.org/0000-0003-0356-6213](https://orcid.org/0000-0003-0356-6213); Email: [oconnor@ice.mpg.de](mailto:oconnor@ice.mpg.de)

**Lorenzo Caputi** – Department of Natural Product Biosynthesis, Max Planck Institute for Chemical Ecology, Jena 07745, Germany; Email: [lcaputi@ice.mpg.de](mailto:lcaputi@ice.mpg.de)

### Authors

**Mohamed O. Kamileen** – Department of Natural Product Biosynthesis, Max Planck Institute for Chemical Ecology, Jena 07745, Germany; Centre for Novel Agricultural Products, Department of Biology, University of York, York YO10 SDD, U.K.; [orcid.org/0000-0002-1346-1055](https://orcid.org/0000-0002-1346-1055)

**Matthew D. DeMars II** – Department of Natural Product Biosynthesis, Max Planck Institute for Chemical Ecology, Jena 07745, Germany; [orcid.org/0000-0002-7268-5286](https://orcid.org/0000-0002-7268-5286)

**Benke Hong** – Department of Natural Product Biosynthesis, Max Planck Institute for Chemical Ecology, Jena 07745, Germany

**Yoko Nakamura** – Department of Natural Product Biosynthesis, Max Planck Institute for Chemical Ecology, Jena 07745, Germany; Research Group Biosynthesis and NMR, Max Planck Institute for Chemical Ecology, Jena 07745, Germany

**Christian Paetz** – Research Group Biosynthesis and NMR, Max Planck Institute for Chemical Ecology, Jena 07745, Germany

**Benjamin R. Lichman** – Centre for Novel Agricultural Products, Department of Biology, University of York, York YO10 SDD, U.K.; [orcid.org/0000-0002-0033-1120](https://orcid.org/0000-0002-0033-1120)

**Prashant D. Sonawane** – Department of Natural Product Biosynthesis, Max Planck Institute for Chemical Ecology, Jena 07745, Germany

Complete contact information is available at: <https://pubs.acs.org/10.1021/jacs.2c08107>

### Funding

Open access funded by Max Planck Society.

### Notes

The authors declare no competing financial interest.

## ■ ACKNOWLEDGMENTS

We would like to thank Chloe Langley for useful discussions on this work, Delia Ayled Serna Guerrero, Sarah Heinicke, and Maritta Kunert for assistance with mass spectrometry, and members of the Max Planck Institute for Chemical Ecology Research Green House for providing and taking care of *Nicotiana benthamiana* plants. We gratefully acknowledge the Max Planck Society and the European Research Council (788301) for funding. B.H. acknowledges the Humboldt Foundation.

## ■ ABBREVIATIONS

Cr, *Catharanthus roseus*; Ti, *Tabernanthe iboga*; CrPAS, precondylocarpine acetate synthase; TiPAS1, precondylocarpine acetate synthase 1; TiPAS2, precondylocarpine acetate synthase 2; TiPAS3, precondylocarpine acetate synthase 3; TiDPAS1, dihydro-precondylocarpine acetate synthase 1; TiDPAS2, dihydroprecondylocarpine acetate synthase 2; CrCS, catharanthine synthase; CrTS, tabersonine synthase; TiTabS, tabersonine synthase; TiCorS, coronaridine synthase; FAD, flavin adenine dinucleotide; NAD(P)H, nicotinamide adenine dinucleotide (phosphate); TIC, total ion chromatogram; EIC, extracted ion chromatogram; S.E., standard error

## ■ REFERENCES

- (1) Kutney, J. P.; Karton, Y.; Kawamura, N.; Worth, B. R. Dihydropyridines in synthesis and biosynthesis. IV. Dehydrosecodine, *in vitro* precursor of indole alkaloids. *Can. J. Chem.* **1982**, *60*, 1269–1278.
- (2) Caputi, L.; et al. Structural basis of cycloaddition in biosynthesis of iboga and aspidosperma alkaloids. *Nat. Chem. Biol.* **2020**, *16*, 383–386.
- (3) Farrow, S. C.; et al. Biosynthesis of an Anti-Addiction Agent from the Iboga Plant. *J. Am. Chem. Soc.* **2019**, *141*, 12979–12983.
- (4) Qu, Y.; et al. Solution of the multistep pathway for assembly of corynanthean, strychnos, iboga, and aspidosperma monoterpene indole alkaloids from 19E-geissoschizine. *Proc. Natl. Acad. Sci. U. S. A.* **2018**, *115*, 3180–3185.
- (5) Caputi, L.; et al. Missing enzymes in the biosynthesis of the anticancer drug vinblastine in Madagascar periwinkle. *Science* **2018**, *360*, 1235–1239.
- (6) Buonora, P.; Olsen, J.-C.; Oh, T. Recent developments in imino Diels–Alder reactions. *Tetrahedron* **2001**, *57*, 6099–6138.
- (7) Khuong-Huu, F.; Cesario, M.; Guilhem, J.; Goutarel, R. Alcaloïdes indoliques—CII: Deux nouveaux types d'alcaloïdes indoliques l'ibophyllidine, dérivé du nor-21(+)-pandolane et l'iboxyphyllidine dérivé de l'abeo-21(20→19)(+)pandolane, retirés des feuilles de tabernanthe iboga baillon et de t. subses-silis stapf. *Tetrahedron* **1976**, *32*, 2539–2543.
- (8) Farrow, S. C.; et al. Cytochrome P450 and O-methyltransferase catalyze the final steps in the biosynthesis of the anti-addictive alkaloid ibogaine from *Tabernanthe iboga*. *J. Biol. Chem.* **2018**, *293*, 13821–13833.
- (9) Lavaud, C.; Massiot, G. *Iboga Alkaloids*; Springer International Publishing, 2017; Vol. 105, pp 89–136.
- (10) Reuß, F.; Heretsch, P. Synthetic strategies for the ibophyllidine alkaloids. *Nat. Prod. Rep.* **2021**, *38* (4), 693–701.
- (11) Zeches, M.; Debray, M. M.; Ledouble, G.; Le Men-Olivier, L.; Le Men, J. Alcaloïdes du *Pandaca caducifolia*. *Phytochemistry* **1975**, *14*, 1122–1124.
- (12) Fishbein, M.; et al. Evolution on the backbone: Apocynaceae phylogenomics and new perspectives on growth forms, flowers, and fruits. *Am. J. Bot.* **2018**, *105*, 495–513.
- (13) Langley, C.; et al. Expansion of the catalytic repertoire of alcohol dehydrogenases in plant metabolism. *bioRxiv* **2022**, DOI: 10.1101/2022.07.24.501124, (accessed 24.07.2022).

(14) Cocquet, G.; Rool, P.; Ferroud, C. A catalytic versus stoichiometric photoinduced electron transfer promoted selective C<sub>16</sub>-C<sub>21</sub> bond cleavage of catharanthine. *Tetrahedron Lett.* **2001**, *42*, 839–841.

(15) Andriamialisoa, R. Z.; Langlois, N. L. Y.; Langlois, Y. Preparation of 15-oxo-16-methoxycarbonyl-15, 20-dihydro-cleavamine and coupling reaction with vindoline. *Heterocycles* **1981**, *1*, 245–250.

(16) Stout, D. M.; Meyers, A. I. Recent advances in the chemistry of dihydropyridines. *Chem. Rev.* **1982**, *82*, 223–243.

(17) Stavrinides, A.; et al. Structural investigation of heteroyohimbine alkaloid synthesis reveals active site elements that control stereoselectivity. *Nat. Commun.* **2016**, *7*, 12116.

(18) Pluskal, T.; et al. The biosynthetic origin of psychoactive kavalactones in kava. *Nat. Plants* **2019**, *5*, 867–878.

(19) Beatty, J. W.; Stephenson, C. R. J. Synthesis of (–)-Pseudo-tabersonine, (–)-pseudovincadifformine, and (+)-coronaridine enabled by photoredox catalysis in flow. *J. Am. Chem. Soc.* **2014**, *136*, 10270–10273.

## Recommended by ACS

### Development of a P450 Fusion Enzyme for Biaryl Coupling in Yeast

Lara E. Zetsche, Alison R. H. Narayan, *et al.*

OCTOBER 31, 2022  
ACS CHEMICAL BIOLOGY

READ 

### Structural Basis of Stereospecific Vanadium-Dependent Haloperoxidase Family Enzymes in Napyradiomycin Biosynthesis

Percival Yang-Ting Chen, Bradley S. Moore, *et al.*

AUGUST 19, 2022  
BIOCHEMISTRY

READ 

### Biocatalytic Carbene Transfer Using Diazirines

Nicholas J. Porter, Frances H. Arnold, *et al.*

MAY 13, 2022  
JOURNAL OF THE AMERICAN CHEMICAL SOCIETY

READ 

### Transamidation-Driven Molecular Pumps

Lorna Binks, David A. Leigh, *et al.*

AUGUST 18, 2022  
JOURNAL OF THE AMERICAN CHEMICAL SOCIETY

READ 

Get More Suggestions >